J Solid State Electrochem (2009) 13:407–416
DOI 10.1007/s10008-008-0567-6

ORIGINAL PAPER

Electrochemical oxidation and determination of ceftriaxone on a glassy carbon and carbon-nanotube-modified glassy carbon electrodes

S. Majdi · A. Jabbari · H. Heli · H. Yadegari · A. A. Moosavi-Movahedi · S. Haghgoo

Received: 20 January 2008 / Accepted: 19 April 2008 / Published online: 27 May 2008

Abstract The electrochemical behavior of ceftriaxone was investigated on a carbon-nanotube-modified glassy carbon (GC-CNT) electrode in a phosphate buffer solution, pH= 7.40, and the results were compared with those obtained using the unmodified one [glassy carbon (GC) electrode]. During oxidation of ceftriaxone, an irreversible anodic peak appeared, using both modified and unmodified electrodes. Cyclic voltammetric studies indicated that the oxidation process is irreversible and diffusion-controlled. The number of electrons exchanged in the electrooxidation process was obtained, and the data indicated that ceftriaxone is oxidized via a one-electron step. The results revealed that carbon nanotube promotes the rate of oxidation by increasing the peak current. In addition, ceftriaxone was oxidized at lower potentials, which thermodynamically is more favorable. These results were confirmed by impedance measurements. The electron-transfer coefficients and heterogeneous electron-transfer rate constants for ceftriaxone were reported using both the GC and GC-CNT electrodes. Furthermore, the diffusion coefficient of ceftriaxone was found to be 2.74×10^{-6} cm^2 s^{-1}. Binding of ceftriaxone to human serum albumin forms a kind of electroreactive species. The percentage of interaction of ceftriaxone with protein was also addressed. A sensitive, simple, and time-saving differential-pulse voltammetric procedure was developed for the analysis of ceftriaxone, using the GC-CNT electrode. Ceftriaxone can be determined with a detection limit of 4.03×10^{-6} M with the proposed method.

Keywords Ceftriaxone · Carbon nanotube · Human serum albumin · Electrocatalysis · Differential pulse voltammetry

Introduction

Since the discovery of carbon nanotubes (CNTs) by Iijima [1] in 1991, CNTs have been the subject of numerous investigations in chemical, physical, and materials areas due to their novel structural, mechanical, electronic, and chemical properties [2, 3]. Their subtle electronic properties suggest that CNTs have the ability to promote charge-transfer reactions when used as an electrode-modifying material. The electrocatalytic effect of CNTs on the redox behavior of some compounds has been reported [4–8].

Drug analysis has an extensive impact on public health. Electrochemical techniques have been used for the determination of a wide range of drug compounds and include the determination of the drug's electrode mechanism. The redox properties of drugs can provide insight into their metabolic fate, their in vivo redox processes, and their pharmacological activity [9, 10].

Ceftriaxone belongs to a group of antibiotics called the cephalosporins. It is a parenteral cephalosporin that displays a broad spectrum of activity against Gram-negative and Gram-positive pathogens [(a) http://www.drugs.com/

S. Majdi · A. Jabbari (✉) · H. Yadegari
Department of Chemistry, Faculty of Science,
K. N. Toosi University of Technology,
P.O. Box: 16315-1618, Tehran, Iran
e-mail: jabbari@kntu.ac.ir

H. Heli · A. A. Moosavi-Movahedi
Institute of Biochemistry and Biophysics, University of Tehran,
Tehran, Iran

S. Haghgoo
Center of Quality Control of Drug,
Tehran, Iran

MTM/ceftriaxone.html; (b) http://www.answers.com/topic/ceftriaxone]. Cephalosporins comprise the cephem nucleus (Scheme 1) and side-chains at positions 3 and 7, which determine their properties and bioactivity [11]. The electroactivity of cephalosporins in the reduction process stems from the double C=C bond in their dihydrothiazine ring. With the exception of the electrode processes resulting from potentially active groups in substituents R1 and R3 (see Scheme 1), the reduction of these antibiotics results in the elimination of R3 [12] via a mechanism in which the first one-electron transfer is the rate-determining step [13–15]. The use of voltammetric techniques allows reaction peaks to be analyzed, which in turn permits the relatively straightforward determination of kinetic parameters [15]. Along this line, a cathodic stripping voltammetry method has been described for determining ceftriaxone [16–18]. However, few reports have dealt with the oxidation of cephalosporins at solid electrodes and the use of the anodic response for their determination [18–25]. Nevertheless, oxidation of the aminothiazole group, which substituted on the side-chain in position 7 of the cephem ring in some cephalosporins, was reported to enable development of a promising amperometric detection mode for liquid chromatography or possibly other flow analytical procedures [21, 22].

Human serum albumin (HSA) is the most abundant protein in human plasma contributing significantly to the transport and regulation of many endogenous and exogenous ligands [23]. It can transport and reversibly bind many chemicals, including drugs, fatty acids, bilirubin, tryptophan and hormones. HSA can also act as a carrier and offer potential binding sites for different metal ions [26–28].

Recently, we involved on the development and application of the modified electrodes aiming at inspection the electrochemistry of biologically important compounds and ligand binding studies [8, 29–33]. In continuation, in the present work, we studied the electrochemical oxidation of ceftriaxone at glassy carbon (GC) and carbon-nanotube-modified glassy carbon (GC-CNT) electrodes, obtained the kinetic parameters, developed an electroanalytical procedure for quantification of ceftriaxone in biological fluids, and investigated the ceftriaxone–HSA interaction.

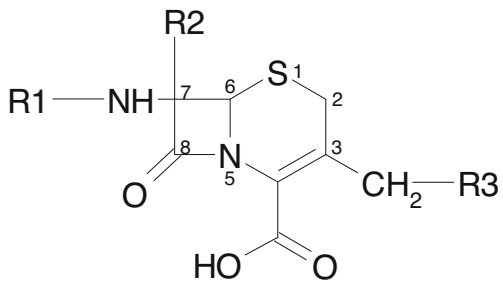

Scheme 1 Chemical structure of cephem nucleus

Experimental

HSA was prepared from Aldrich. Ceftriaxone was obtained as a gift from the Center of Quality Control of Drug, Tehran, Iran. Multiwall CNTs were prepared by chemical vapor deposition, with≈95% purity. All other chemicals used in this work were of analytical reagent grade from Merck.

The standard solution of authentic ceftriaxone was prepared in 100 mM phosphate buffer solution (PBS), pH 7.40 (which was also used as the supporting electrolyte), and then stored in the dark at 4 °C.

Drug-free serum samples were obtained from healthy male volunteers and stored frozen until the assay. The serum samples were diluted (1:7) with the supporting electrolyte and filtrated through a 30 kDa filter to produce protein-free human serum. Various portions of stock ceftriaxone solution were transferred into 10-ml volumetric flasks containing 3.3 ml of the serum sample. These solutions were diluted to the mark with the supporting electrolyte for preparation of spiked samples (final dilution of 1:20 with the supporting electrolyte). The protein-free spiked serum solutions were directly analyzed. Urine samples taken from a healthy person were diluted (1:10) with PBS after adding an appropriate amount of standard ceftriaxone solution. The resulting solution was then directly analyzed.

Electrochemical measurements were carried out in a conventional three-electrode cell, powered by an electrochemical system comprising the Autolab system with PGSTAT30 and FRA2 boards (Eco Chemie, Utrecht, The Netherlands). The system was run on a PC using GPES and FRA 4.9 software. For impedance measurements, a frequency range of 100 kHz to 50 mHz was employed. The AC voltage amplitude used was 10 mV, and the equilibrium time was 5 s. An Ag/AgCl-Sat'd KCl and a platinum disk (from Azar Electrode, Iran) were used as reference and counter electrodes, respectively. The working electrode was either GC or GC-CNT electrodes. For differential pulse voltammetry (DPV) measurements, a pulse width of 25 mV, pulse time of 50 ms, and scan rate of 10 mV s^{-1} were employed.

Before each measurement, the GC electrode was polished on a polishing micro-cloth with 0.5 μM alumina powder and rinsed thoroughly with redistilled water, followed by sonication for 3 min in an ultrasonic bath. The electrode was then transferred to the supporting electrolyte and potential in the range of −100 to 1,700 mV was applied in a regime of cyclic voltammetry (CV) until a stable voltammogram was achieved. Aiming at the modification of the GC surface, first, the CNTs were pretreated as reported previously [34]. Briefly, CNTs were refluxed in a nitric acid solution, washed with redistilled water, and then sonicated

in a 3:1 sulfuric/nitric acid solution in an ultrasonic bath. Before the modification, the GC electrode was polished and then transferred to the 1 M sulfuric acid solution. Potential in the range of −1,000 to 2,000 mV was applied in a regime of CV for 20 cycles. Fifty milligrams of CNTs were dispersed into acetone with the aid of ultrasonic stirring for 6 h. A 10-μl aliquot of this dispersion was dropped on the pretreated GC electrode surface, and the solvent was allowed to dry in air.

The microscopic areas of the GC-CNT and the bare GC electrodes were obtained by CV using 1 mM $K_4Fe(CN)_6$ as a redox probe at different scan rates. For a reversible process, the anodic peak current i_{pa} can be calculated as follows [35]:

$$I_{pa} = \left(2.69 \times 10^5\right) n^{3/2} \mathrm{A}\ \mathrm{C}^*\ D^{1/2} v^{1/2} \quad (1)$$

where I_{pa} refers to the anodic peak current. For $K_4Fe(CN)_6$, n=1 and D=7.6×10^{-6} cm s^{-1} [36]. Therefore, from the slope of the i_{pa} vs. $\nu^{0.5}$ relation, the microscopic areas were determined to be 0.033 cm^2 for the bare GC and 0.081 cm^2 for the GC-CNT electrodes. Evidently, the modified electrode had an increased surface area of nearly 145%.

Surface morphological studies were carried out using scanning electron microscopy (SEM), using a Philips instrument, Model X-30. The transmission electron microscopy (TEM) was performed using a Phillips transmission electron microscope with an accelerating voltage of 80 kV was used to obtain information about the morphology and size of particles.

The solution pH was adjusted using a Metrohm 744 pH meter. All studies were carried out at room temperature.

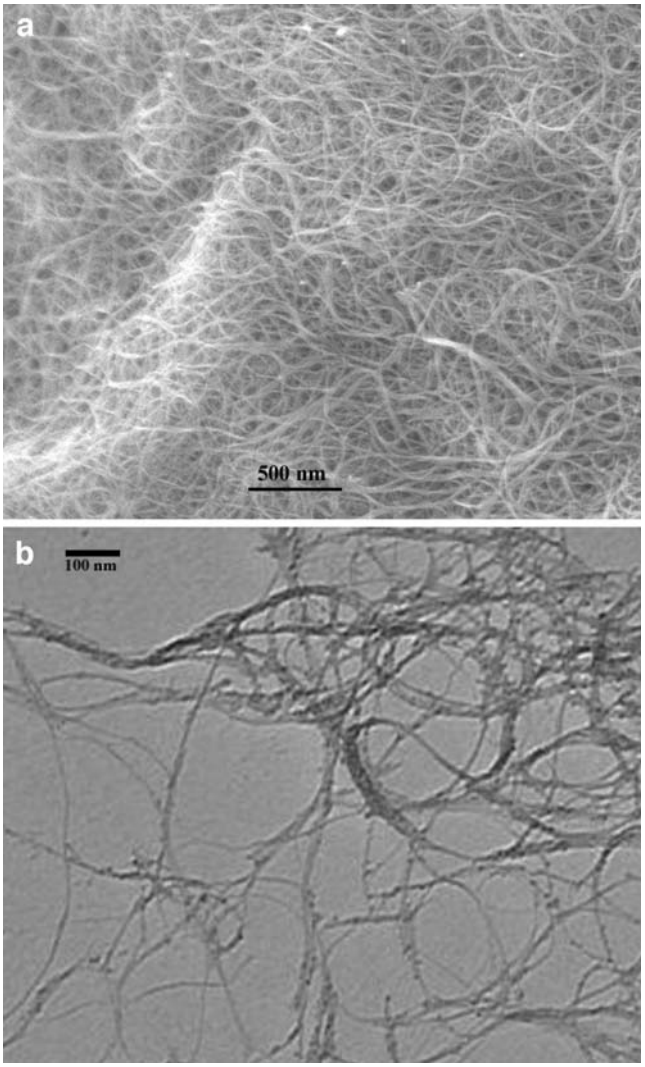

Fig. 1 **a** The scanning electron micrograph of GC-CNT electrode. **b** Transmission electron micrograph of CNTs

Results and discussion

Figure 1A shows the scanning electron micrograph of GC-CNT electrode surface. It can be seen that the CNT's were formed as bundles, some of which twisted together. They formed a homogeneous film on the electrode surface. Figure 1B represents the transmission electron micrograph of CNTs. It can be observed that they have an average diameter of 10–30 nm and of 500–1,000 nm length.

Figure 2B shows typical cyclic voltammograms of 6.0 mM ceftriaxone in PBS using GC (a) and GC-CNT (b) electrodes. One anodic peak appeared in each voltammogram, with potentials of 915 and 865 mV using the GC and GC-CNT electrodes, respectively, at a potential sweep rate of 100 mV s^{-1}. In the reverse sweep, however, no peaks appeared, indicating an irreversible heterogeneous electron-transfer process for the oxidation of ceftriaxone. The peak current obtained using the GC-CNT electrode increased considerably with respect to that obtained using the bare GC electrode, and the corresponding potential shifted to more negative values. Therefore, modification of the electrode surface with CNTs produced an enhancement of the electrochemical oxidation response, and CNTs also catalyzed the oxidation process. This effect has been also observed previously [4–8, 34, 37, 38]. The catalytic efficiency of CNT can be attributed to the nanometer dimensions of the CNTs that are homogeneously and stably distributed and assembled on a GC electrode and that most of the adsorbed CNTs are in the form of small bundles or single tubes. Each assembled nanotube is fully and easily accessible to analytes and, consequently, can be readily and completely used as an electrochemical sensing unit, yielding a higher sensitivity. Moreover, CNTs have a particular electronic structure, high electrical conductivity, and topological defects present on their surfaces [39], which may have caused the electrocatalytic efficiency during the electrooxidation process [4–8].

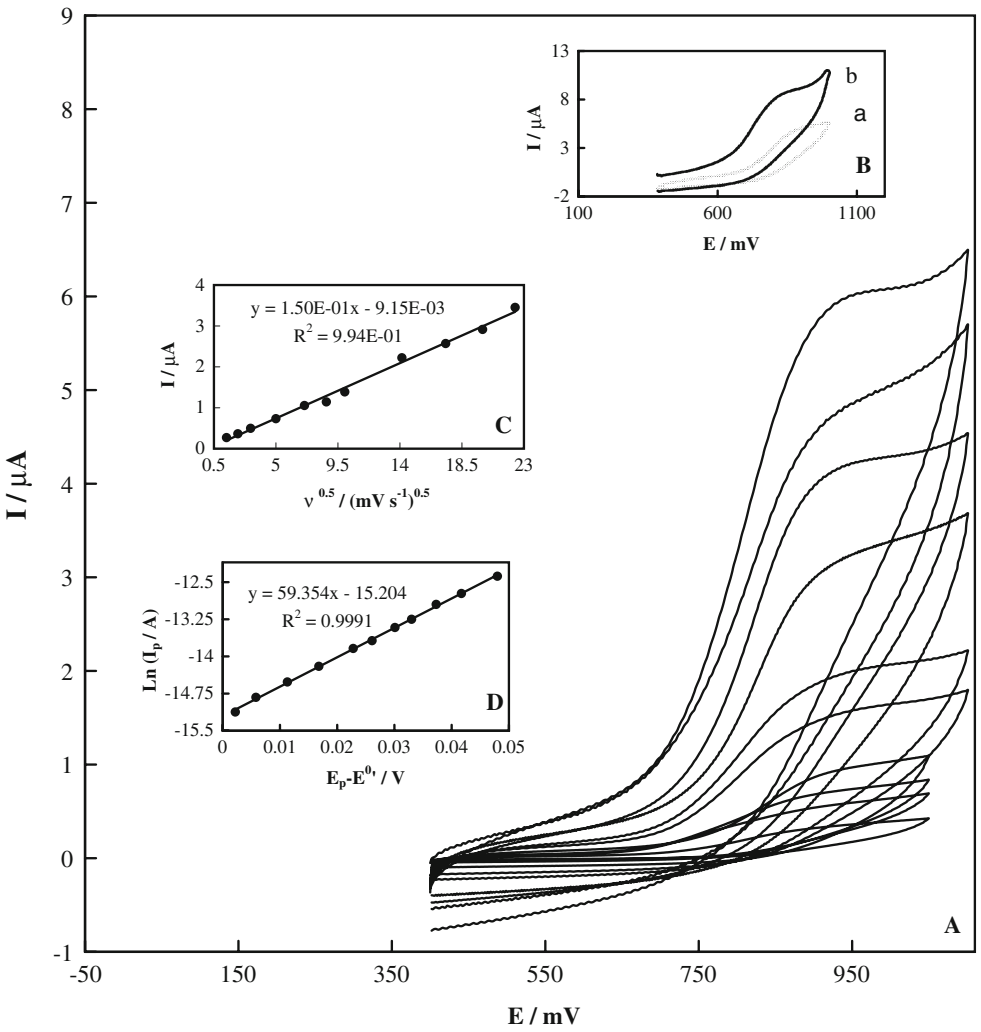

Fig. 2 **A** Cyclic voltammograms for PBS containing 6.0 mM ceftriaxone using the GC electrode recorded at different potential sweep rates. Potential sweep rates from inner to outer are 2, 5, 10, 25, 50, 75, 100, 200, 300, 400, and 500 mV s^{-1}. **B** Cyclic voltammograms of PBS containing 6.0 mM ceftriaxone using GC (*a*) and GC-CNT (*b*) electrodes. Potential sweep rate was 100 mV s^{-1}. **C** Dependency of peak current on the corresponding square root of potential sweep rate. **D** Dependency of natural logarithm of peak current on ($E_p - E^{0,}$)

Controlled-potential coulometry was performed in PBS containing 0.6 mM ceftriaxone using both electrodes at 1,040 mV; a similar experiment was performed in ceftriaxone-free solution. The electrolysis progress was monitored by CV. The extrapolated charge consumption for total electrolysis of the solution, after corrections for background/charging currents, was derived, and the number of exchanged electrons for each anodic peak was found to be one. Therefore, ceftriaxone oxidized on both the GC and GC-CNT surfaces via one one-electron step. A similar voltammogram, accompanied by the same number of exchanged electrons, was reported for cefepime [40]. It has been reported [40] that aminothiazole moiety can be oxidized and an anodic peak can generated. The anodic peak appearing in the voltammogram can be related to the oxidation of this functional group.

The effect of potential sweep rate was studied using the GC electrode in the range of 2 to 500 mV s^{-1}. Along with the potential sweep rate increase, the peak current increased and the peak potential shifted to more positive values (Fig. 2A), confirming the irreversible nature of the reaction processes. In addition, the peak currents depend linearly on the corresponding square root of the potential sweep rate (Fig. 2C). This result indicates that a mass transport phenomenon has occurred via diffusion in the oxidation process. From the slope of the linear dependency of the anodic peak current on the square root of the potential sweep rate and using the Randles–Sevcik equation for totally irreversible electron-transfer processes [41]:

$$I_p = \left(2.99 \times 10^5\right) n\alpha^{0.5} A\, C^*\, D^{0.5} \nu^{0.5} \quad (2)$$

where α is the electron-transfer coefficient, n is the number of exchanged electron, A is the surface area of the working electrode, C^* and D are the bulk concentration and diffusion coefficient of the electroreactant species, respectively, and ν is the potential sweep rate; the diffusion coefficient of ceftriaxone has been obtained as 2.74×10^{-6} cm^2 s^{-1}, using α=0.45 (vide infra). It should be noted that the values of the diffusion coefficients obtained using

both electrodes are nearly the same, since diffusion of the electroreactant species in the bulk of the solution does not depend on the target surface in a semi-infinite linear diffusion process.

For irreversible diffusion-controlled processes, the peak potential is proportional to ln I_p within the following equation [41]:

$$I_p = 0.227\, nFAC^* k^0 \exp\left[-\alpha F/RT\left(E_p - E^{0,}\right)\right] \quad (3)$$

where I_p, k^0 and $E^{0,}$ are the peak current, standard rate constant and formal potential (obtained from extrapolation of the peak current to the potential sweep rate of zero), respectively. Figure 2D represents the dependency of ln I_p vs. $(E_p - E^{0,})$, obtained from the voltammograms recorded at various potential sweep rates using the GC electrode. Using this plot and based on Eq. 3, the values of the electron-transfer coefficient and standard rate constant were obtained as 0.45 and 3.62×10^{-3} cm s^{-1}, respectively. Similar voltammograms were collected for ceftriaxone using the GC-CNT electrode. The values of the electron-transfer coefficient and standard rate constant using the modified electrode were obtained as 0.68 and 3.55×10^{-3} cm s^{-1}, respectively. Therefore, CNT increases the rate of the electrooxidation process of ceftriaxone ≈ 10 times, due to its electrocatalytic activity [4–8] related to the nanostructure effect of CNT (vide supra).

Figure 3 shows the Nyquist diagrams of the GC electrode, recorded at 100 mV as DC-offset for different concentrations of ceftriaxone in PBS as are the Nyquist diagrams obtained from the fitting of the experimental data on the equivalent circuit (vide infra). The Nyquist diagrams represent two overlapped, slightly depressed capacitive semicircles. The high-frequencies semicircle is related to the electron-transfer process and so the combination of charge-transfer resistance and double-layer capacitance. The low-frequencies semicircle can be related to an adsorption process [42], which is the adsorption of the reaction's intermediate(s) on the electrode surface. The adsorption of reaction intermediates on the electrode surface can create capacitance or inductive loops in the Nyquist diagrams [42, 43]. Therefore, the low-frequencies semicircle can be characterized by the parallel combination of a capacitance and a resistance related to the capacitive character of the adsorption process and a related faradaic resistance.

It should be noted that the diffusion process observed during the oxidation process (Fig. 3, inset a) probably would have appeared at very low frequencies with a high time constant in relatively low concentrations of ceftriaxone; it did not appear in the sweeping frequency range in the Nyquist diagrams. The Nyquist diagram recorded at high concentrations of ceftriaxone represents a linear tail (Fig. 3, inset), with a slope of near unity at very low frequencies. This linear tail, which appeared only in the high concentrations, was attributed to the semi-infinite diffusion of the electro-reactant species [44], which was also observed in

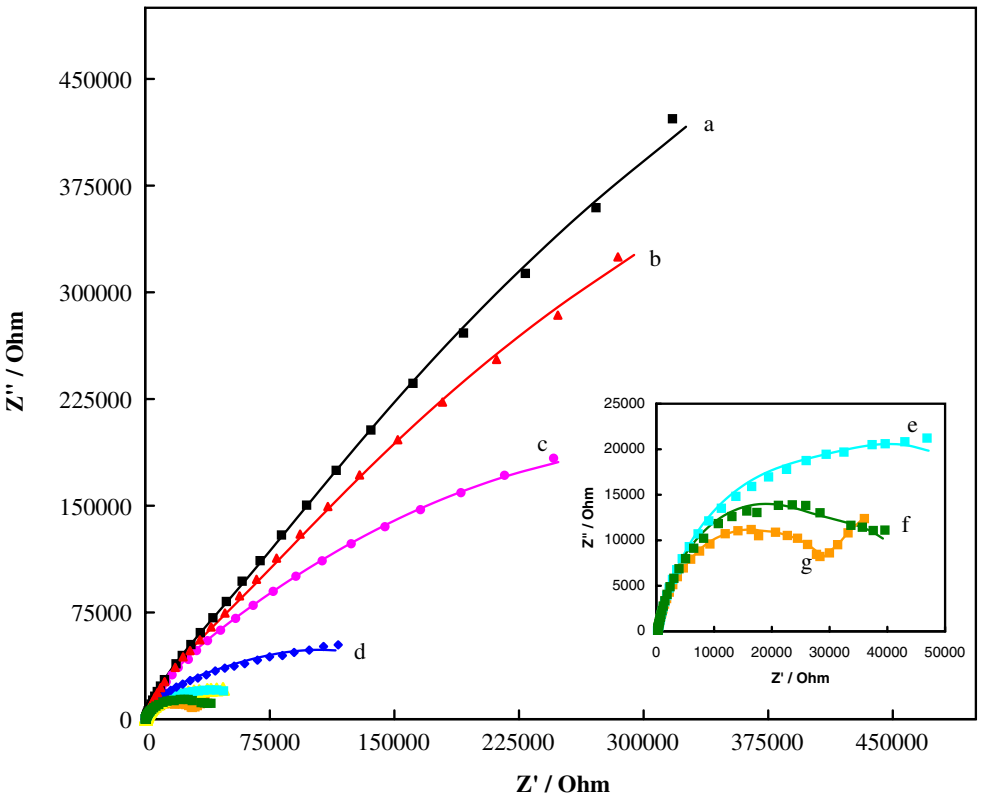

Fig. 3 Main panel: Nyquist diagrams of PBS containing different concentrations of ceftriaxone: *a* 1×10^{-5}, *b* 5×10^{-5}, *c* 1×10^{-4}, *d* 5×10^{-4}, *e* 1×10^{-3}, *f* 5×10^{-3}, *g* 1×10^{-2} M using GC electrode recorded at 100 mV. *Inset* Nyquist diagram recorded at high concentrations of ceftriaxone

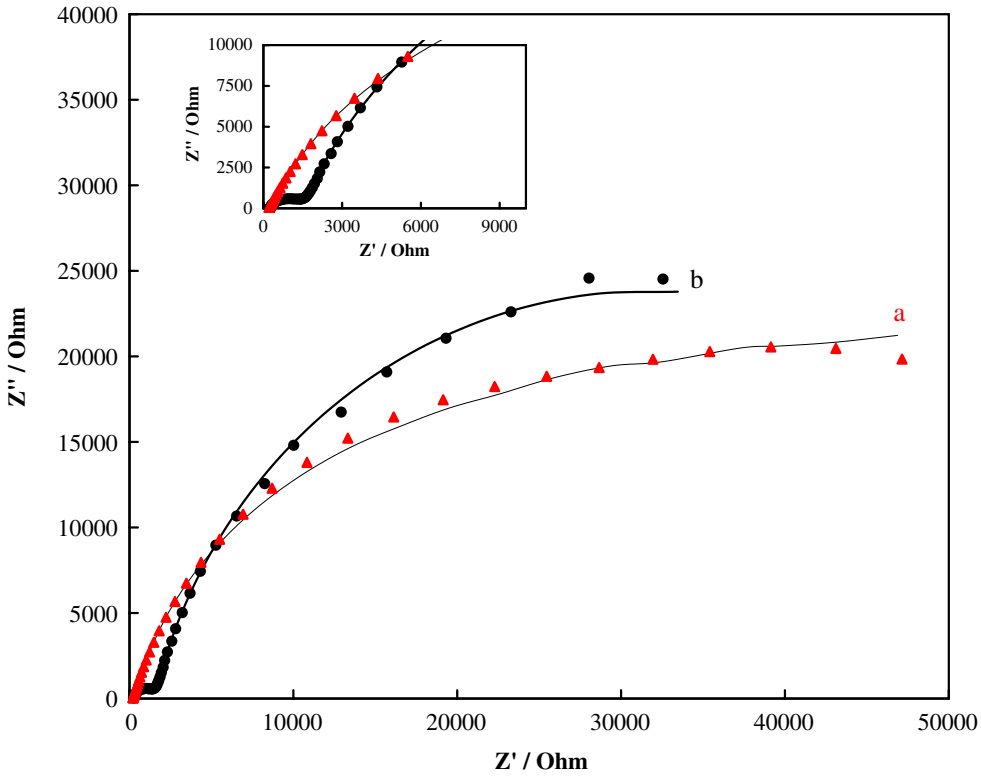

Fig. 4 Nyquist diagrams of PBS containing 1 mM ceftriaxone using GC (*a*) and GC-CNT (*b*) electrodes. Bias in both diagrams was 100 mV

the regime of cyclic voltammetry (see Fig. 3, inset a). The equivalent circuit compatible with the Nyquist diagrams represented in Fig. 4 is depicted in Scheme 2. In this electrical equivalent circuit, R_s, CPE_{dl} and R_{ct} represent solution resistance, a constant phase element corresponding to the double-layer capacitance and the charge-transfer resistance, respectively. In addition, R_{ads} and C_{ads} signify surface adsorption resistance and a capacitance representing the adsorption process. W, which is included in the circuit only at high concentrations of ceftriaxone, is the Warburg element related to the semi-infinite diffusion process that appeared in high concentrations of ceftriaxone. Table 1 shows the values of the equivalent circuit elements obtained by fitting the experimental results. The goodness of the fit can be judged by the estimated relative errors presented in the parentheses. In Table 1, T_0 and n are the CPE impedance coefficient and exponent, respectively. According to the values of the electrical equivalent elements reported in this table, upon increasing the concentration of ceftriaxone, the charge-transfer and adsorption resistances decreased due to the facile occurrence of the faradaic process related to the electrooxidation process, while the adsorption capacitance values increased. Moreover, the concentration of ceftriaxone had little effect on the double-layer capacitance.

Figure 4 shows the Nyquist diagrams of GC (A) and GC-CNT (B) electrodes recorded at 100 mV as dc-offset for

Table 1 The values of the elements in equivalent circuit and the corresponding relative errors shown in Scheme 2 fitted in the Nyquist plots of Fig. 3

	CPE_{dl}					
R_s (Ω)	$T_0 \times 10^6$ (Ω^{-1} s^n cm^{-2})	n	R_{ct} (Ω cm^2)	C_{ads} (μF cm^{-2})	R_{ads} (Ω cm^2)	C (mM)
214.3 (1.28%)	31.9 (2.41%)	0.95 (0.38%)	5,348.0 (0.87%)	47.0 (3.99%)	68,544.3 (2.29)	0.01
213.8 (1.26%)	33.8 (2.38%)	0.95 (0.38%)	4,735.5 (5.02%)	61.2 (3.88%)	48,480.3 (2.19%)	0.05
212.7 (0.40%)	40.0 (1.11%)	0.94 (0.17%)	4,166.6 (5.39%)	91.6 (2.51%)	18,534.8 (6.04%)	0.10
213.6 (0.58%)	40.0 (1.62%)	0.94 (0.25%)	1,871.07 (4.46%)	217.1 (3.64%)	4,519.4 (4.96%)	0.50
209.6 (0.63%)	45.4 (1.57%)	0.91 (0.25%)	1,534.24 (2.41%)	247.4 (1.43%)	650.0 (1.58%)	1.00
209.4 (1.20%)	43.9 (2.34%)	0.94 (0.38%)	1,157.44 (2.58%)	676.5 (3.95%)	386.9 (4.98%)	5.00
211.1 (1.43%)	42.0 (2.27%)	0.93 (0.38%)	968.72 (1.68%)	691.0 (4.47%)	87.2 (4.27%)	10.0

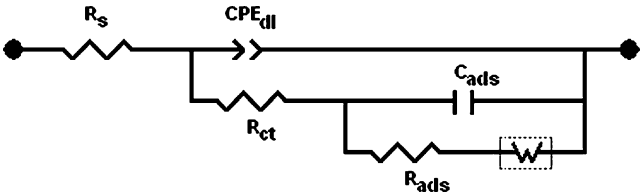

Scheme 2 Electrical equivalent circuit compatible with the Nyquist diagrams shown in Figs. 3 and 4

1 mM ceftriaxone in PBS. The Nyquist diagrams obtained by fitting the experimental data on the equivalent circuit depicted in Scheme 2 are also illustrated. In both diagrams, two slightly depressed semicircles have appeared related to the charge-transfer resistance of the electrooxidation and the adsorption of reaction intermediate(s) processes. The diffusion process that occurred during the oxidation process using both electrodes probably had a very large time constant and did not appear in the Nyquist plot. The values of the equivalent circuit elements obtained by fitting the experimental results are shown in Table 2, accompanied by the estimated relative errors. In Table 2, the charge-transfer resistance related to the oxidation process using the GC-CNT electrode is much smaller than that obtained using the GC electrode. Considering the effect of the real surface area of both electrodes (the GC-CNT electrode has a surface area≅2.5 times larger than that of the GC electrode), a value of≅13 times smaller for the charge-transfer resistance indicates the higher charge-transfer rate for oxidation of ceftriaxone on the GC-CNT electrode surface, due to the electrocatalytic effect of CNT on the electrooxidation process. Moreover, comparison of the values of R_{ads} obtained for the GC and GC-CNT electrodes (see Table 2) indicates that CNT increased the resistance toward adsorption of the reaction intermediate(s). Therefore, CNTs reduce the affect of adsorption and result in voltammograms with higher reproducibility. This effect will be seen to be more positive when we analyze the application of the modified electrode. Similar results have been also observed previously for the electrooxidation and determination of other drug [8].

The interaction of ceftriaxone with HSA was also investigated, using CV and the GC electrode. We did not use the GC-CNT electrode to investigate this interaction due to the possible adsorption of HSA on the CNT surface. Figure 5 shows the voltammograms of PBS containing 0.5 mM ceftriaxone in the absence (a) and presence of (b) 0.0393 μM HSA added to the solution. When HSA was added to the ceftriaxone solution, the peak currents of ceftriaxone decreased, the peak potential shifted to more positive values, and no new peaks appeared in the potential window. Moreover, the peak currents depend linearly on the square roots of the potential sweep rate (data not shown). These results indicate that interaction between ceftriaxone and HSA has occurred and that the bound form of ceftriaxone remains electroreactive (it should be noted that the concentration of HSA added to the ceftriaxone solution is high enough to bind all ceftriaxone molecules). Therefore, it can be deduced that ceftriaxone interacts with HSA and that the resulting macromolecule is electroreactive in the swept potential, which has a smaller diffusion coefficient with respect to the free ceftriaxone. The interaction between a ligand such as ceftriaxone with HSA yields a macromolecular ensemble whose size is notoriously larger than the free ligands. Therefore, it is expected that interaction will result in an equilibrium decrease in the diffusion coefficient for the ceftriaxone-HSA molecules.

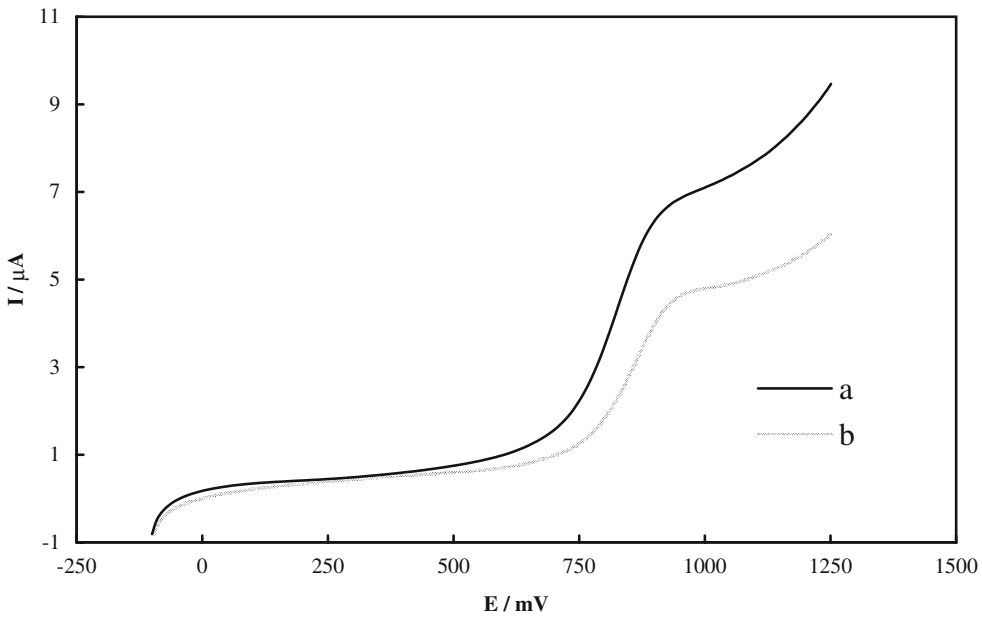

Fig. 5 Typical voltammograms of PBS containing 0.5 mM ceftriaxone in the absence (*a*) and presence of (*b*) 0.0393 μM HSA added to the solution

Table 2 The values of the elements in equivalent circuit and the corresponding relative errors shown in Scheme 2 fitted in the Nyquist plots of Fig. 4

	CPE_{dl}					
R_s (Ω)	$T_0 \times 10^4$ (Ω^{-1} s^n cm^{-2})	n	R_{ct} (Ω cm^2)	C_{ads} (μF cm^{-2})	R_{ads} (Ω cm^2)	Electrode
209.6 (0.63%)	45.4 (1.57%)	0.91 (0.25%)	1,534.24 (2.41%)	247.4 (1.43%)	650.0 (1.58%)	GC
210.1 (0.53%)	42.9 (3.44%)	0.87 (0.52)	116.48 (0.83%)	575.9 (0.49%)	4,884.0 (1.19%)	GC-CNT

To confirm that the lowering of peak currents is due to the interaction of ceftriaxone with HSA and not to an increase in the solution viscosity, cyclic voltammograms were recorded in the buffer solution containing $K_4Fe(CN)_6$ in the absence and presence of HSA, using the GC electrode, as it is well known that $Fe(CN)_6^{4-}$ does not interact with HSA [45]. In the absence and presence of HSA, two well-defined peaks were observed, with the same cathodic and anodic peak potentials and currents that decreased only a little in the presence of HSA. This indicates that HSA had only a minimal effect on the solution viscosity.

The Randles–Sevcik equation can be rearranged for quasi-reversible electrode kinetics as follows, assuming that the interaction of ceftriaxone-HSA is a dynamic equilibrium phenomenon [46, 47]:

$$I_p = 2.99 \times 10^5 A\, n\, \alpha^{0.5} C_t (x_b D_b + x_f D_f)^{0.5} v^{0.5} \quad (4)$$

In this equation, I_p, A, D_f, D_b, C_t, and ν are the peak current, electrode surface area, diffusion coefficient of free species, diffusion coefficient of bound species, analytical concentration of ceftriaxone, and potential sweep rate, respectively. Also, x_b and x_f are the mole fractions for the bound and free species, respectively. Equation 4 indicates that both free and bound ceftriaxone participated in the peak current in the voltammogram (b) depicted in Fig. 5. Furthermore, in this equation, D_b is assumed to be equal to the diffusion coefficient of HSA (6.28×10^{-7} cm^2 s^{-1} [48]) and α is assumed to remain intact. Accordingly, the mean value of x_b was obtained as 0.615; therefore, the percentage of interaction acquired was 61.5%.

The applicability of DPV as an analytical method for the determination of ceftriaxone was examined by measuring the peak current as a function of concentration of the bulk drug. The dependency existing between peak current and concentration of the drug was rectilinear using both the GC and GC-CNT electrodes. The analytical characteristics of ceftriaxone in PBS using both electrodes are reported in Table 3. As can be seen, the slope of the calibration graph for the determination of ceftriaxone in PBS using the GC-CNT electrode is ≅6.6 times greater than for the bare GC electrode, while the electrode surface area is ≅2.5 times greater. This result is due to the electrocatalytic effect of CNT on the electrooxidation of ceftriaxone (Fig. 2B). The limits of detection (LOD) and quantitation (LOQ) of the procedure were calculated according to the 3 and 10 SD/m criteria, respectively, where SD is the standard deviation of the intercept and m is the slope of the calibration curves [49]. The LOD and LOQ are reported in Table 3; their values confirm the sensitivity of the proposed procedure for the determination of ceftriaxone. The precision of the method is calculated as the relative standard deviation.

The applicability of the proposed method for the determination of ceftriaxone in biological fluids was examined by measuring the peak current as a function of the bulk concentration of the drug in both the urine and serum samples using the GC-CNT electrode. The generally

Table 3 Results obtained for ceftriaxone analysis from spiked human serum and urine samples using GC and GC-CNT electrodes

Medium	GC-CNT	GC-CNT	GC	GC-CNT
	Serum	Urine	Buffer	Buffer
Linearity range (M)	1.00×10^{-4}–1.00×10^{-3}	3.00×10^{-5}–9.09×10^{-4}	5.00×10^{-5}–1.00×10^{-3}	2.00×10^{-5}–1.00×10^{-3}
Slope [$\mu A(mM)^{-1}$]	22.3	6.56	1.98	13.1
Correlation coefficient (r)	0.997	0.995	0.994	0.995
RSD (%)[a]	3.44	3.52	3.05	2.93
LOD (M)	1.98×10^{-5}	1.06×10^{-5}	8.78×10^{-6}	4.03×10^{-6}
LOQ (M)	6.60×10^{-5}	2.40×10^{-5}	2.92×10^{-5}	1.34×10^{-5}
Recovery (%)[b]	98.0	99.6	99.5	99.7

[a] Each value is obtained from seven experiments.
[b] Recovery value is the mean of seven experiments.

poor selectivity of voltammetric techniques can pose problems in the analysis of biological samples, which contain oxidizable substances. However, no current due to oxidation of the compounds appeared in either the serum or urine samples. The results obtained from our proposed technique for determining ceftriaxone in serum and urine samples are listed in Table 3. The percentage recovery of ceftriaxone was determined by comparing the peak currents of a known drug concentration in both media with their equivalents in calibration curves; these results are also summarized in Table 3. Good recoveries of ceftriaxone were achieved from these matrices, meaning that the application of our proposed voltammetric method to the analysis of ceftriaxone in biological fluids can be easily assessed.

Conclusion

The electrochemical behavior and electrocatalytic oxidation of ceftriaxone was studied in the PBS, pH 7.4, on GC and GC-CNT electrodes, using electrochemical techniques. The kinetic parameters such as the transfer coefficient (α), the standard rate constant (k^0), and the diffusion coefficient (D) for oxidation of ceftriaxone were determined using the proposed method. The kinetics of ceftriaxone oxidation on the modified surface was enhanced and the oxidation process performed at thermodynamically favorable potentials, beyond the effect of real surface area enhancement. This electrocatalytic effect was attributed to the nano-size, special electronics, and structure of CNT. Furthermore, an adsorption process occurred during the redox process of ceftriaxone on the electrode surface, revealed by impedance measurements; although this process was weakened when using the modified surface. The determination of protein-binding ability toward ceftriaxone through voltammetric measurements of the diffusion coefficients resulted in a reproducible and simple methodology. The evaluation of the percentage of interaction through voltammetric measurements allows its calculation, regardless of the nature of the interaction between ceftriaxone and proteins. It is possible to apply this methodology when covalent, electrostatic, or van der Waals bounds are present, and the equipment involved in the measurements is quite simple. A DPV procedure was optimized and successfully applied for quantification of ceftriaxone in bulk form and human biological fluids. The simplicity, sensitivity, selectivity, and short time of analysis are the main advantages of these procedures, making them useful for routine analysis.

Acknowledgment The financial support of the Research Council of K. N. Toosi University of Technology and University of Tehran are gratefully acknowledged.

References

1. Iijima S (1991) Nature 354:56
2. Ajayan PM (1999) Chem Rev 99:1787
3. Balasubramanian K, Burghard M (2005) Small 1:180
4. Qu FL, Yang MH, Lu YS, Shen GL, Yu RQ (2006) Anal Bioanal Chem 386:228
5. Wu KB, Wang H, Chen F, Hu SS (2006) Bioelectrochemistry 68:144
6. Huang H, Zhang W, Li MC, Gan YP, Chen JP, Kuang YF (2005) J Colloid Interface Sci 284:593
7. Gooding JJ (2005) Electrochim Acta 50:3049
8. Yadegari H, Jabbari A, Heli H, Moosavi-Movahedi AA, Karimian K, Khodadadi A (2008) Electrochim Acta 53:2907
9. Wang J (ed) (1996) Electroanalytical techniques in clinical chemistry and laboratory medicine. VCH, New York
10. Ozkan SA, Uslu B, Aboul-Enein HY (2003) Crit Rev Anal Chem 33:155
11. Garzone P, Lyon J, Yu VL (1983) Drug Zntell Clin Pharm 17:507
12. Gchiai M, Aki O, Morimoto A, Okada T, Shinozaki K, Asahi Y (1974) J Chem Soc Perkin Trans 1:258
13. Hall DA (1973) J Pharm Sci 62:980
14. Hall DA, Berry DM, Schneider CJ (1977) J Electroanal Chem 80:155
15. Munoz E, Avila JL, Camacho L, Cosano JE, Garcia-Blanco F (1988) J Electroanal Chem 257:281
16. El-Maali NA, Ali AMM, Khodari M, Ghandour MA (1991) Bioelectrochem Bioenerg 26:485
17. Altinoz S, Temizert A, Beksac SB (1990) Analyst 115:873
18. Ogorevc B, Krasna A, Hudnik V, Gomiscek S (1991) Mikrochim Acta 1:131
19. Bishop E, Hussein W (1984) Analyst 109:913
20. Ivaska A, Nordstrom F (1983) Anal Chim Acta 146:87
21. Fabre H, Blanchin MD, Tjaden U (1986) Analyst 111:1281
22. Fabre H, Blanchin MD, Kok W (1988) Analyst 113:651
23. Billova S, Kizek R, Jelen F, Novotna P (2003) Anal Bioanal Chem 377:362
24. Hammam E, EL-Attar MA, Beltagi AM (2006) J. Pharm Biomed Anal 42:523
25. Altinöz S, Özer D, Temizer A, Yüksel N (1994) Analyst 119:1575
26. He XM, Carter DC (1992) Nature 358:209
27. Yamazaki E, Inagaki M, Kurita O, Inoue T (2005) J Biosci 30:475
28. Shen X-C, Liang H, Guo J-H, Song C, He X-W, Yuan Y-Z (2003) J Inorganic Biochem 95:24
29. Majdi S, Jabbari A, Heli H (2007) J Solid State Electrochem 11:601
30. Hajjizadeh M, Jabbari A, Heli H, Moosavi-Movahedi A, Haghgoo S (2007) Electrochim Acta 53:1766
31. Heli H, Moosavi-Movahedi AA, Jabbari A, Ahmad F (2007) J Solid State Electrochem 11:593
32. Heli H, Sattarahmady N, Jabbari A, Moosavi-Movahedi AA, Hakimelahi GH, Tsai F-Y (2007) J Electroanal Chem 610:67
33. Hajjizadeh M, Jabbari A, Heli H, Moosavi-Movahedi AA, Shafiee A, Karimian K (2008) Anal Biochem 373:337
34. Yadegari H, Jabbari A, Heli H, Moosavi-Movahedi AA, Karimian K, Khodadadi A (2008) Electrochimica Acta 53:2907
35. Bard AJ, Faulkner LR (2001) Electrochemical Methods. Wiley, New York, p 231
36. Wang SF, Xu Q (2006) Bioelectrochem 71:1
37. Goyal RN, Tyagi A, Bachheti N, Bishnoi S (2008) Electrochimica Acta 53:2802
38. Antoniadou S, Jannakoudakis D, Theodoridou E (1989) Synth Met 30:295
39. Britto PJ, Santhanam KSV, Rubio A, Alonso JA, Ajayan PM (1999) Adv Mater 1(1):154

40. Ozkan SA, Uslu B, Zuman P (2002) Anal Chim Acta 457:265
41. Bard AJ, Faulkner LR (2001) Electrochemical methods. Wiley, New York, p 236
42. Majdi S, Jabbari A, Heli H, Moosavi-Movahedi AA (2007) Electrochim Acta 52:4622
43. Jafarian M, Mahjani MG, Heli H, Gobal F, Khajehsharifi H, Hamedi MH (2003) Electrochim Acta 48:3423
44. Barsoukov E, Macdonald JR (2005) Impedance spectroscopy. Wiley, New Jersey
45. Moulton SE, Barisci JN, Bath A, Stella R, Wallace GG (2003) J Colloid Interface Sci 261:312
46. Carter MT, Rodriguez M, Bard AJ (1989) J Am Chem Soc 111:8901
47. Grover N, Gupta N, Singh P, Thorp HH (1992) Inorg Chem 31:2014
48. Peters T (1996) All about Albumin. Academic, San Diego
49. Miller JC, Miller JN (1994) Statistics for analytical chemistry, 4th edn. Ellis-Harwood, New York